

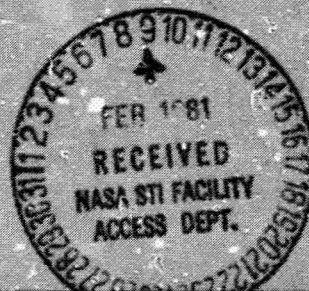
(NASA-CR-163886) STUDY OF FOLDABLE ELASTIC
TUBES FOR LARGE SPACE STRUCTURE APPLICATIONS
Final Report, Feb. - Dec. 1980 (Howard
Univ.) 46 p HC A03/MF A01

CSCL 22B

N81-16080

Unclas

G3/14 41150



DEPARTMENT OF CIVIL ENGINEERING
HOWARD UNIVERSITY
WASHINGTON, D. C.

Howard University

STUDY OF FOLDABLE ELASTIC TUBES FOR
LARGE SPACE STRUCTURE APPLICATIONS
FINAL REPORT
For
PHASE II

by

Irving W. Jones
Caster D. Williams

January 1981

Conducted Under NASA Grant NSG 1320

Principal Investigator:

Irving W. Jones
Professor, Civil Engineering
Howard University

NASA Technical Officer:

Joseph E. Walz
Structures and Dynamics Division
Langley Research Center

PREFACE

The research reported herein is a continuation of work reported earlier in ref. 1, and was conducted at Howard University under NASA Grant NSG 1320: Graduate Research Program in Advanced Aerospace Structures during the period February 1980 through December 1980.

Supervisor for this project was Dr. Irving W. Jones. The work has been monitored by Dr. G. C. Horner and Mr. Joseph E. Walz of Langley. Assisting in this phase of the work have been graduate assistants Caster D. Williams and Steve O. Mitchell, and undergraduate assistant Thomas Green.

The laboratory work was performed under the direct supervision of Mr. William B. Steward, engineering technologist, who also collaborated with Dr. Jones on the design of the FET testing machine and prepared the working drawings. Vendors who provided materials and services are named in various sections of the report.

A separate report, ref. 2, is being submitted to the Office of Research Grants and University Affairs, LaRC, which chronicles the general progress of the Graduate Research Program, with emphasis on the progress and accomplishments of the participating students since the program began.

ABSTRACT

This report presents the results of Phase II of an investigation of a type of foldable structural member that might be suitable for use in self-deploying space structures; specifically, structures which deploy through the use of released strain energy.

Phase I of this investigation, documented in an earlier report (ref. 1), consisted of the design and fabrication of a set of foldable elastic tube test specimens, the design and construction of a special-purpose testing machine to measure the deployment characteristics, performance of the first series of tests, and an analysis of the test results. All of the tasks leading up to the testing were accomplished with generally satisfactory results. The specimens of the first test series, however did not deploy (unfold) successfully, but instead, settled into a partially buckled state just as they had almost completed the unfolding action. This result corroborated the conclusion of an earlier investigation conducted elsewhere. (ref. 5)

The continuation of the study from that point, which has consisted of making various modifications to the tube design, re-testing the tubes and analyzing the new results has been defined as Phase II of the study. It has been completed and is reported herein.

One type of modified tube, referred to as the slotted tube, deployed successfully and reliably, and has become the focus of the continued work.

Establishment of optimal design criteria, taking into consideration deployment as well as strength and buckling behavior, is the ultimate objective of this project.

TABLE OF CONTENTS

	<u>Page</u>
Preface	i
Abstract	ii
1. INTRODUCTION	
1.1 Background	1
1.2 Scope and Objectives	3
2. TEST SPECIMENS	
2.1 Geometry	4
2.2 Material and Fabrication	8
2.3 Slot Configurations	10
3. FOLDING ELASTIC TUBE TESTING MACHINE	
3.1 Design	12
3.2 Operation	12
4. TEST PLAN	
4.1 Background: Test Results from Phase I	16
4.2 Deployment Test Procedure	18
5. TEST RESULTS	
5.1 Free-Edged Tube	19
5.2 Single-Slotted Tube	19
5.3 Double-Slotted Tube	23
5.4 Approximate Strain Energy - Geometry Relationship	24
5.5 Some Design-Related Parameters as Approximated by Formula	25
6. Conclusion	37
References	38
Appendix A: Typical Form Block Drawing	39
Appendix B: Quasi-Static Analysis - FET Testing Machine	40

ILLUSTRATIONS

<u>Figure</u>	<u>Page</u>
1.1 Bi-convex Foldable Elastic Tube (BFET)	2
2.1 Test Specimen Geometry	5
2.2 Modified BFET Configurations.	7
3.1 Assembly Drawing/FET Testing Machine	13
3.2 FET Testing Machine in Operation	14
3.3 FET Testing Machine Instrumentation	15
4.1 Plot of Bending Moment vs. Angle for Tube Settling with Buckled State	17
5.1 Modified BFET Test Specimens (Photographs)	20
5.2 Plot of Bending Moment vs Angle for Tube with 1/16" Single Slot	21
5.3 Stress Alleviation Slot	22
5.4 - 5.11 Plots of Bending Moment vs. Angle for Various Single-Slotted Tubes	26-33
5.12 - 5.14 Plots of Strain Energy vs. Various Parameters as Approximated by Formula	34-36

TABLES

<u>Number</u>	<u>Page</u>
2.1 Test Specimen Data	6
2.2 Armco 17-7PH Stainless Steel Properties	9
5.1 Bending Stiffness Related to Slot Config- uration	34

1. INTRODUCTION

1.1 Background

The foldable structural members being studied in this investigation are among candidate types for use in so-called "strain-energy deployable" truss structures; that is, a type of truss structure which can be folded up into a dense package with some members being folded sharply in half, remaining elastic and thus storing strain energy. The folded structure is restrained in this configuration for launch into space, whereupon it is released to deploy through the utilization of the stored strain energy.

The particular type of foldable member investigated here is one which has been called in some previous literature a bi-convex foldable elastic tube (BFET), a closed thin-walled cylindrical tube made up of circular cylindrical segments joined to form the shape shown in Fig. 1.1. Earlier research on the BFET has been reported in refs. 1, 3, 4 and 5. The concept of employing as a foldable member a tube whose cross-section can be flattened and thus remain elastic is attractive because of its simplicity. It dispenses with the need for a mechanical hinge or spring. However, despite early optimistic results with this type of tube (ref. 3), in the most recent study cited above, ref. 5, and in the present study, it has demonstrated a serious shortcoming. That is that in many instances when the tube has almost completed its unfolding action and is within about 15 degrees of becoming straight, and the previously flattened center region is snapping back and to its original shape, the tube settles into a state of stable equilibrium in a slightly buckled configuration. Ref. 5, which documents an extensive experimental and theoretical investigation of the BFET, reported repeated occurrences of this phenomenon, and gives a theoretical proof of the existence of such a buckled equilibrium state. Ref. 1

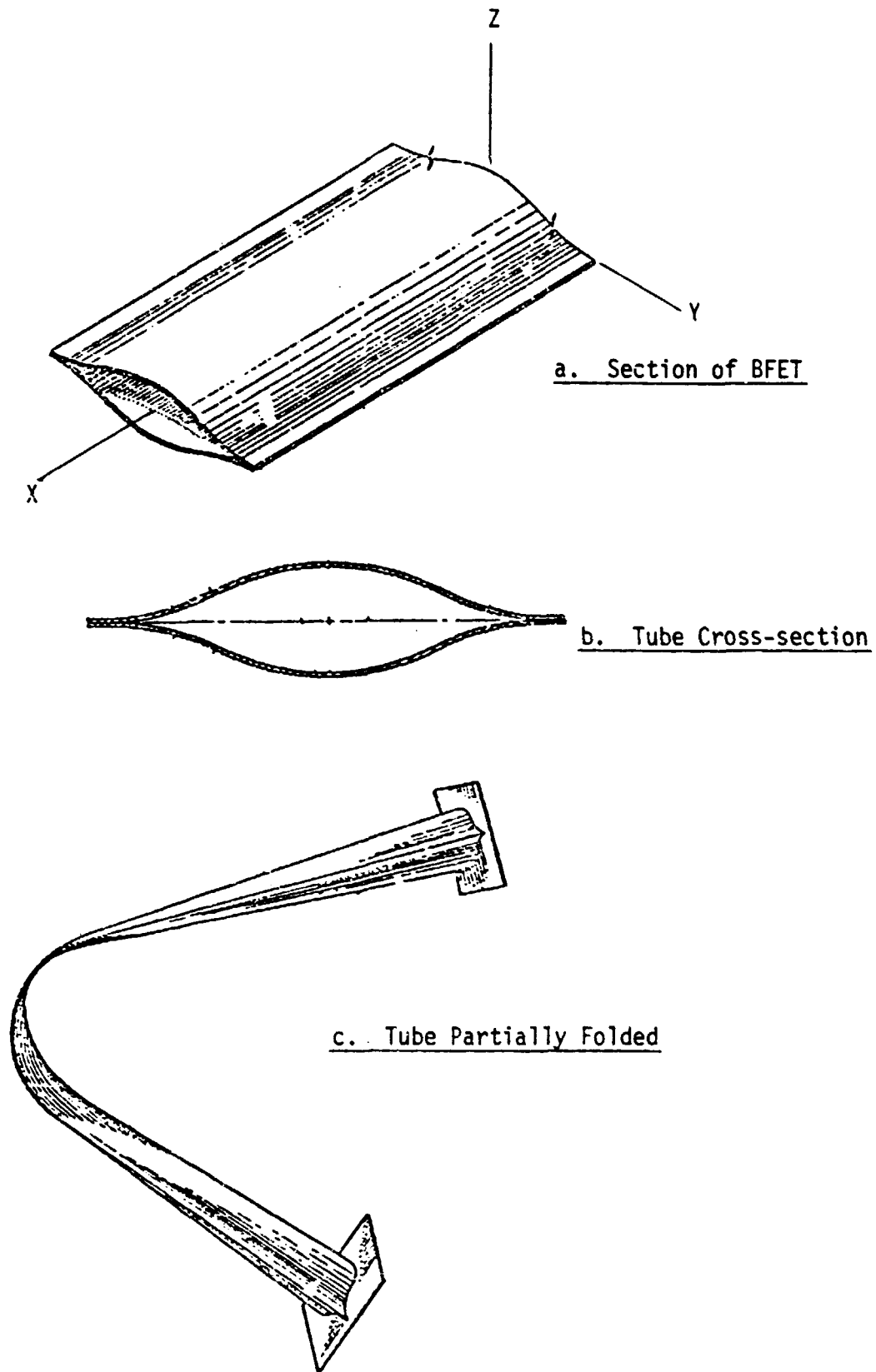


Fig. 1.1 Bi-Convex Foldable Elastic Tube (BFET)

which reports on phase I of the present project, cites further examples of this behavior, which imply the need for a design modification or abandonment of the design.

1.2 Scope and Objectives

This report contains the results of making various modifications to the BFET in an effort to eliminate the buckling problem. It was found that by cutting narrow slots in the central region of the tube, in the longitudinal (x , in Fig. 1.1a) direction, the buckled state could be avoided and the tube would deploy completely. These slots serve to relieve the high compressive strains that develop in the tube in the lateral (y) direction as its center region attempts to snap through. After discovering that this approach was successful, the objective of subsequent work was to determine the optimum width, length and location for the slots and the sacrifice in strength and stiffness due to their insertion, to re-test the tube specimens under the same conditions as was previously done, and to analyze the test results in order to relate the strain energy released to the tube geometry mathematically. The results of these efforts are detailed in sections 2 through 5 of the report. Some material from ref. 1 is repeated here in order to make this report a complete and independent documentation of the project to date.

2. TEST SPECIMENS

2.1 Geometry

When the six circular arcs forming the cross-section of the BFET are identical, as is the case in this study, the cross-section shape can be uniquely defined by any two of the parameters R , λ and f , shown in Fig. 2.1a. For this analysis, the independent parameters were chosen as R , the arc radius, and f , a measure of the tube flatness, which is defined as $f = \lambda/R$, where λ is the offset of the circular arc center from the mid-plane. The value of f can vary from 0 to 1, with the extremes being $f = 0$ (a cross-section whose central portions is round) and $f = 1$ (a completely flat cross-section).

For this investigation, it was desired to have an array of 30 to 40 shapes varying in both size and in flatness, but having the same wall thickness, $t = 0.010$ inches, and length, $L = 48$ inches.

The wall-thickness, length and range of cross-section sizes were all established such that the test specimens would represent the center region of an actual large space truss member, as it is expected to be proportioned, according to some preliminary NASA studies (e.g., ref. 6). The folding in a 15' to 20' member would be expected to take place well within the 48" length that was assigned to those specimens (Fig. 2.1 lb).

Due to (1) inaccuracies in forming of the specimen halves by the rubber pad process, (2) small changes in shape that occurred when the specimens were handled for seam welding, and (3) further small changes in the heat treating process, the specimens, when ready for testing, did not have exactly the cross-section contours that were originally designed. But, as can be seen from Table 2.1, the set of 33 specimens covered a wide enough range of radii ($1.41" < R < 5.91"$) and flatnesses ($0.07 < f < 0.89$), to satisfy the original goals in those categories. As is shown, the specimens were categorized into

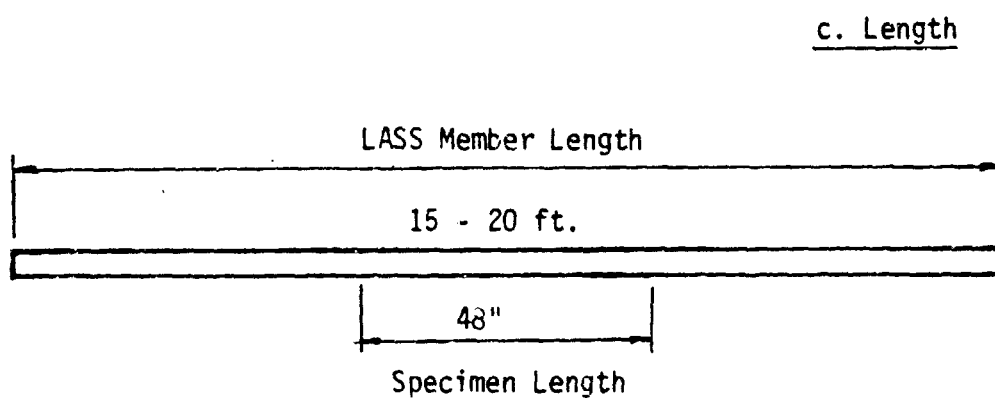
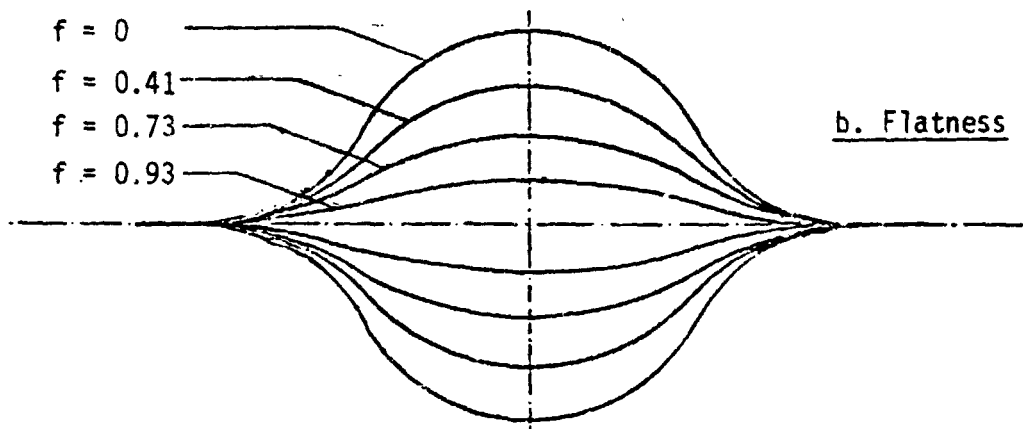
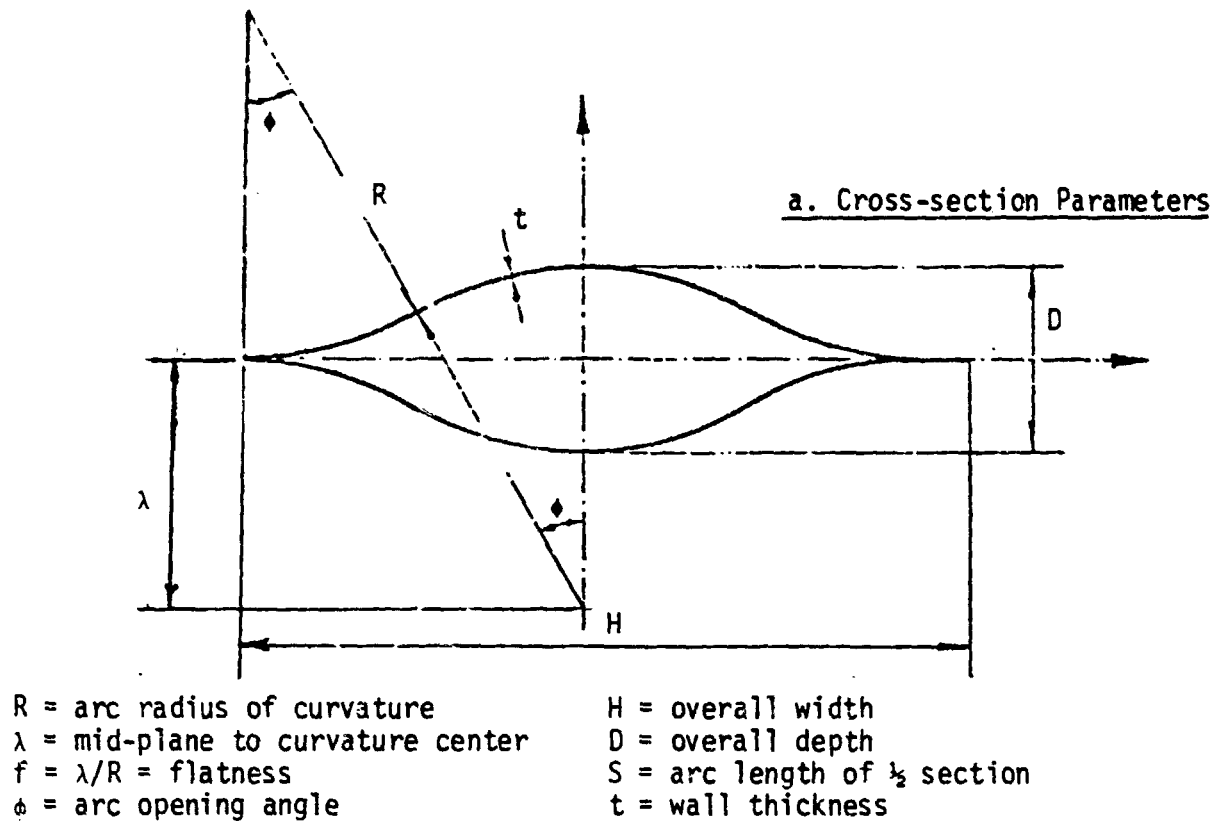


Fig. 2.1 TEST SPECIMEN GEOMETRY

TABLE 2.1
TEST SPECIMEN DATA

Specimen No.	Radius, R in.	Offset, λ in.	Flatness, f	Slot Configuration (See Fig. 2-2)	M- θ Curve included in this report
VERY FLAT					
NA-1	5.91	5.27	0.89	SS	Fig. 5-4 Fig. 5-5
NA-2	5.71	5.04	0.88	SS	
NB-1	3.58	2.85	0.80	SS	
NB-2	3.45	2.65	0.77	SS	
NB-3	3.76	2.57	0.68		
NB-4	3.53	2.38	0.67		
NB-5	3.56	2.23	0.63		
MODERATELY FLAT					
NC-1	1.80	1.08	0.60	SS	Fig. 5-6
NC-2	1.82	1.05	0.58	FE	
NC-3	1.88	1.02	0.54	DS	
ND-1	1.65	0.82	0.50	SS	Fig. 5-2 Fig. 5-8
ND-2	1.80	0.89	0.49		
ND-3	1.76	0.85	0.48	FE	
NE-1	2.76	1.42	0.51	SS	
NE-2	2.71	1.16	0.43		
NE-3	2.49	1.55	0.61	FE	
NF-1	1.50	0.79	0.52	SS	Fig. 5-9
NF-2	1.58	0.69	0.44	FE	
NF-3	1.56	0.67	0.43	SS	
NF-4	1.57	0.66	0.42	SS	
NF-5	1.41	0.53	0.38		
NF-6	1.54	0.57	0.37		
SLIGHTLY FLAT					
NG-1	2.03	0.65	0.32	FE	Fig. 5-10
NG-2	2.00	0.57	0.28	SS	
NG-3	2.40	0.82	0.34		
NG-4	2.14	0.59	0.27	SS	
NG-5	2.42	0.40	0.16	SS	
NG-6	2.50	0.49	0.20	FE	
ROUND					
NH-1	2.00	0.35	0.17	DS	Fig. 5-11
NH-2	2.21	0.36	0.16	FE	
NH-3	2.10	0.20	0.09		
NH-4	1.86	0.18	0.10		
NH-5	1.66	0.12	0.07	SS	

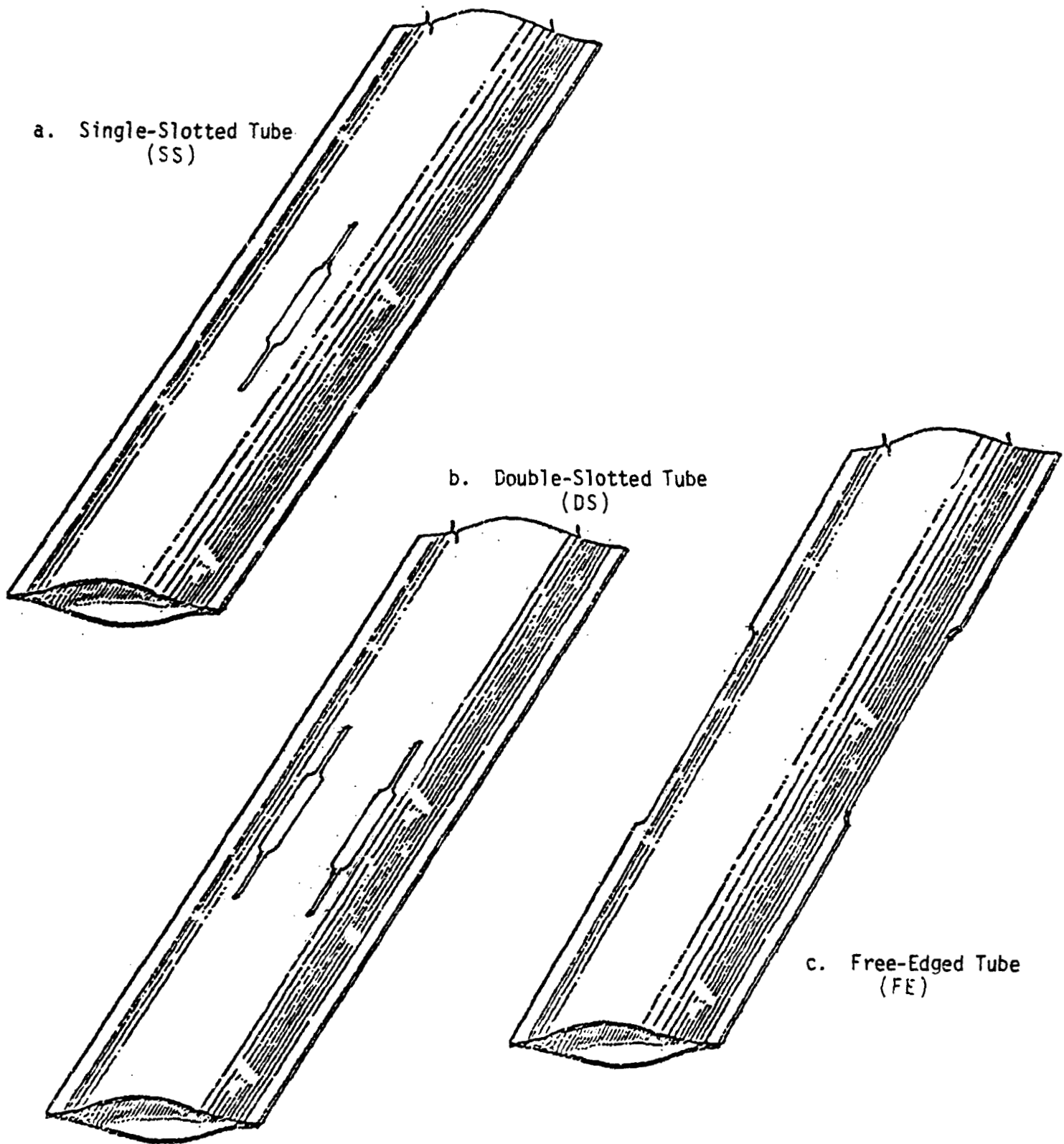


Fig. 2.2 MODIFIED BFET CONFIGURATIONS

groups with similar radii (R) and offsets (λ). Thus, they could be given identifications according to group (NA through NH) indicating general size and degree of flatness, the cross-section properties having been measured directly from penciled outlines of the specimen ends.

2.2 Material and Fabrication

The success of the foldable elastic tube concept depends upon the tube remaining elastic throughout when it is folded sharply in half through 180° . Therefore, the tube must be made of a material with high yield strain (high yield stress and/or low modulus of elasticity). Also, fabrication and strength-to-weight considerations dictate that the material have adequate formability, weldability and low density. The material chosen for this study, a stainless steel, possesses all of these qualities, as do titanium, some hard copper alloys and composites. The selected material, Armco 17-7PH stainless, proved to be satisfactorily formable in the annealed condition and hardenable to sufficiently high strength levels by the use of a standard heat treatment. Fabrication practices for 17-7PH are the same as for other chromium-nickel stainless steels. Specified mechanical properties at room temperature, as well as properties determined from tests on the material used in this project are shown in Table 2.2. To obtain the latter, standard tensile coupons were cut from sheets of the 17-7PH material that had been subjected to the heat-treatment along with the test specimens. These were tested and the results were as shown. The yield strengths averaged 179,500 and 189,500 psi in the direction of roll and transverse direction respectively. The yield strength in the roll direction was a little below the supplier's specified value of 185,000 psi, but was sufficiently high for our purposes (See ref. 7).

The specimen halves were formed by the Guerin, or rubber pad, process.

TABLE 2.2
ARMCO 17-7PH STAINLESS STEEL PROPERTIES

SPECIFIED MECHANICAL PROPERTIES, ROOM TEMPERATURE				
Typical Properties				
Condition	Ultimate Tensile Strength, psi (Mpa)	0.2% Tensile Yield Strength psi (Mpa)	Elongation % in 2" (50 mm)	Hardness, Rockwell
ANNEALED	130,000 (896)	40,000 (276)	35	B85
TH1050	200,000 (1379)	185,000 (1276)	9	C43
RH950	235,000 (1620)	220,000 (1517)	6	C48

PROPERTIES OF MATERIAL USED IN THIS INVESTIGATION				
Condition	Ultimate Tensile Strength, psi (Mpa)	0.2% Tensile Yield Strength psi (Mpa)	Elongation % in 2" (50 mm)	Hardness, Rockwell
ANNEALED	Longitudinal:			
	146,000 (1006)	54,000 (372)	31	B75
	Transverse:			
	146,000 (1006)	53,000 (365)	28	B75
TH1050	Longitudinal:	179,500		
	Transverse:	189,500		

Rubber pad forming employs either a monolithic or layered rubber pad encased in a heavy retainer. The pad acts in the manner of the recessed part of a die. A form block acts as the punch in conventional forming. The block is secured either to the ram or the platen of the press. The blank (the piece to be formed) is positioned between the form block and the rubber pad, and as the two are brought together, the blank is forced into the rubber pad and is bent into the shape of the form block. The rubber acts somewhat like a hydraulic fluid in exerting nearly equal pressure over the surface of the blank.

The forming set-up was as follows. A multi-layered rubber pad was encased in the steel retainer box. The box was supported on two steel horses which were already available in the laboratory. Above, the precisely contoured form block was secured to the 4' x 4' head plate of the 600,000 lb. capacity universal testing machine, which was utilized as the press. Each rectangular sheet, or blank, was positioned on the form block by inserting its two locating holes into the corresponding two locating pins (one at each end) on the block. The blank was lubricated with drawing wax prior to fastening. As the press was lowered, the blank was formed into the shape of the block; upon removal of the pressure, it sprang back to a shape of lesser curvature. The form blocks were designed with shapes such that, theoretically, the specimen half should relax into the originally planned shape after spring-back. A typical form-block is shown in Appendix A.

2.3 Slot Configurations

The idea of cutting slots in the tubes suggested itself during observations of the earlier tests on the closed tubes (ref. 1). It appeared that some type of stress alleviation device was needed to remedy the buckling problem. Slotting the tubes makes the snap-through phase of deployment

easier by reducing the compressive strains and stresses in the lateral direction, due to the insertion of free edges.

The arrangements of the slots were established in such a way that the tubes might both deploy fully and maintain sufficient bending stiffness. Three configurations, as shown in Fig. 2.2, were conceived. For convenience, these are referred to in later sections of the report as follows:

- . Free-Edged (FE) - The seam weld and material 1/16 inch inside it cut away to produce free edges on upper and lower halves of tube.
- . Single-Slotted (SS) - One slot cut on each side (compression and tension (or +Z and - Z) sides of tube along its center-line, or X - X axis.
- . Double Slotted (DS) - Two slots cut on each (+Z and - Z) sides of tube along the line of tangency of the circular cylindrical sections.

The workability of these three configurations, as well as the required width and length of the slots was investigated through an incremental process. Initially, the slots in the single and double-slotted tubes were made 1/16 inch wide, and for all three configurations the incisions were eight inches long. Although the slots are needed only on the side of the tube that is in compression when folded, they were cut on both sides to preserve symmetry and local buckling resistance.

The slots were cut into the tubes by mounting the tube in a milling machine, with a mandril (pipe) placed inside for internal support, and then cutting the slots with carbide mill ends.

3. FET TESTING MACHINE

3.1 Design

An assembly drawing of the testing machine is shown in Fig. 3.1 and photographs of it in Fig. 3.2. As is shown, the machine has two arms, one fixed and one which rotates, hinged at a central vertical shaft: The arms are each approximately $5\frac{1}{2}$ feet long, and are made of rectangular aluminum tubing. The central fittings comprising the hinge are made of machined aluminum and are installed in ball bearings for minimum friction. This assembly rests on a supporting stand, and the arm rotates in a horizontal plane. Near the outboard end of each arm is a mounting plate onto which a specimen end piece (insert) is attached. The specimen is thus firmly situated horizontally between the mounting plates. This upper assembly is attached to the arms by flex plates, which permit the specimen to extend uninhibited in its longitudinal (X) direction. Appendix B shows the quasi-static force distribution through various sections, and the specimen under a pure bending moment.

3.2 Operation

With the arms in the extended configuration and the test specimen bolted to the plates, the tube is completely flattened in the center region, and the specimen (along with the movable arm) is rotated through 180^0 . The reaction against the stationary arm is sensed by a load cell mounted against it near the outboard end. The shaft of the movable arm is connected below to a variable speed gear drive that was installed to regulate the rate of unfolding. A magnetic clutch mounted on the shaft permits completely free release of the specimen when this mode is desired.

As the specimen unfolds and the resisting force is measured by the load cell, an angular displacement transducer simultaneously measures the angle of rotation. The signals from these instruments actuate an x-y recorder which

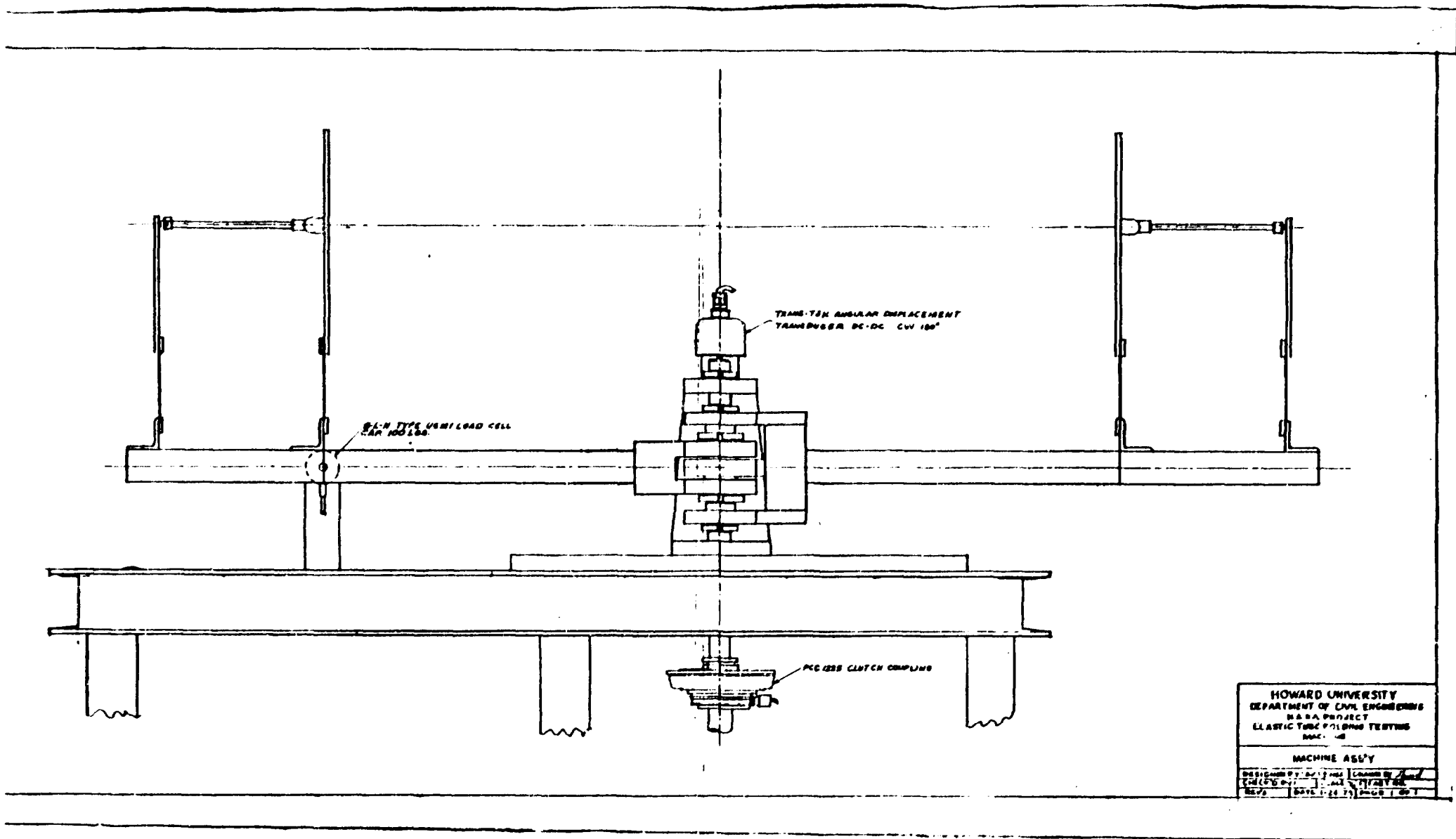
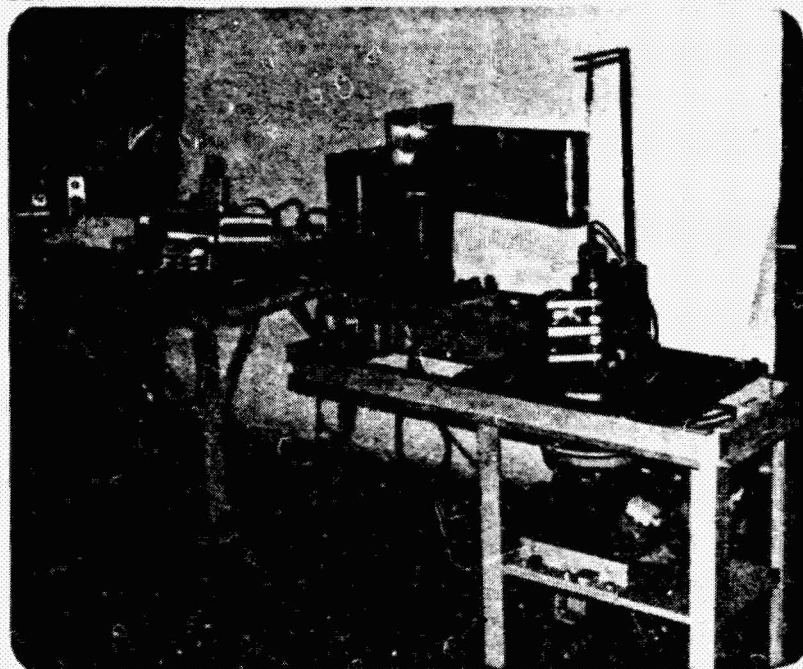


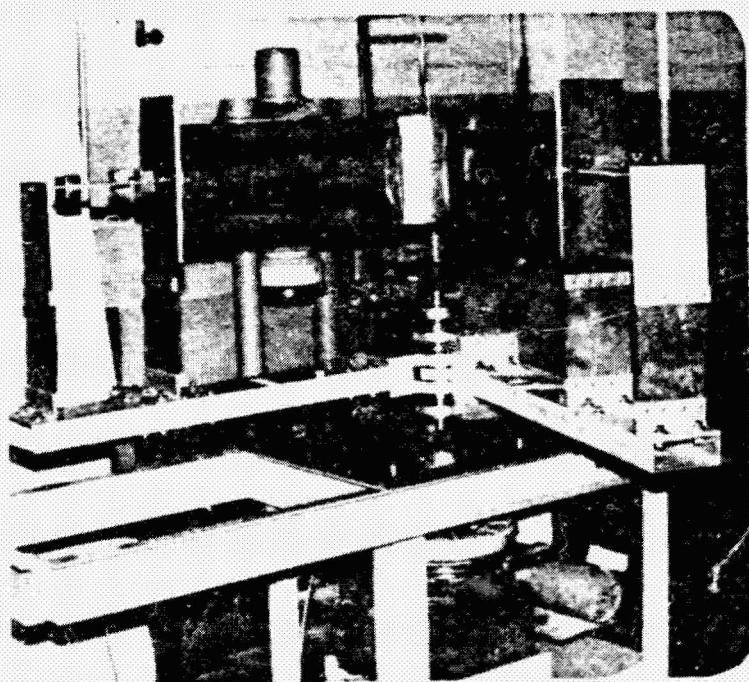
Fig. 3.1

Assembly Drawing FET Testing Machine

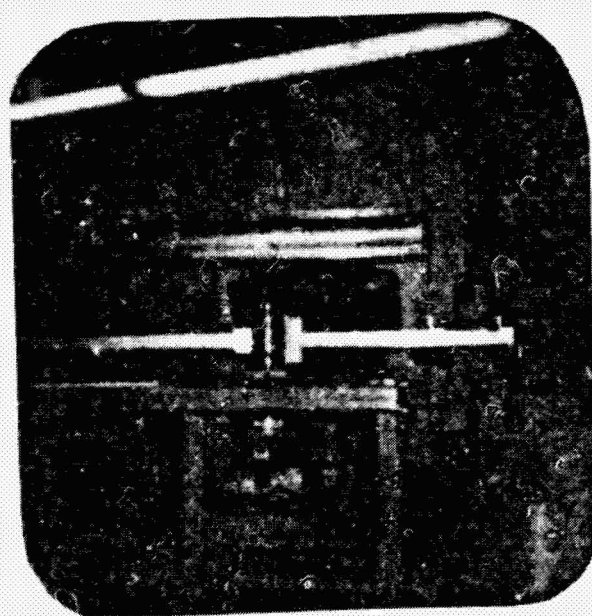
plots the force vs. angle curve. Instrumentation is shown in Fig. 3.3.



a. Folded



b. Partially Deployed



c. Fully Deployed

Fig. 3.2 FET Testing
Machine in Operation

ORIGINAL PAGE 37
DATE 10-12-1966

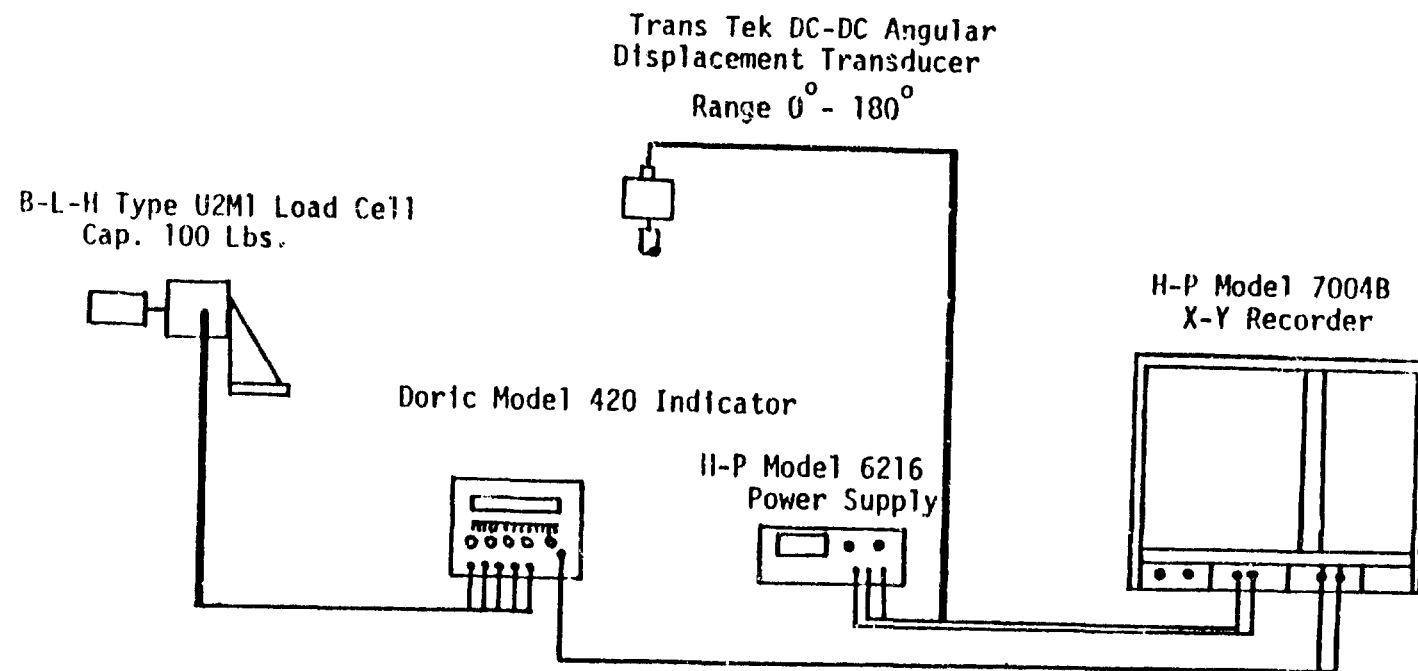


Fig. 3.3 Elastic Tube Folding Machine Instrumentation

4. TEST PLAN

4.1 Background: Test Results from Phase I

In Phase I of this project, tests were performed on seven specimens (six different shapes), and results are presented in ref. 1. The specimens were tested an average of three times each at different angular velocities. In every case the tube was folded as compactly as possible with the two halves parallel and in contact. The fold radii were recorded.

The result of the test series was that only two of the seven specimens deployed fully. The other specimens came to rest (in self-equilibrium) in some bent position. The tubes, however, remained elastic and could be pushed back out to their original shapes by the experimenter, and re-tested. There were some small wrinkles after the first test. The same behavior repeated itself on these five tubes in subsequent tests. A typical moment versus angle curve for a tube behaving in this manner is shown in Fig. 4.1, where it can be seen that equilibrium is reached when the tube is at a angle of about 10° . These results are presented in detail in ref. 8.

The only tube which both deployed fully, and remained sound structurally, was one of the flattest ($f = 0.78$). One of the rounder ones ($f = 0.42$), exhibited a different behavior. It failed to deploy fully at first, but later deployed completely, but by this time the material in the center region showed cracks on the compression side.

Our major conclusion from this series of tests was that generally, this type of tube is subject to settle into a slightly bent position, with the compression side of the center region not completely expanding to its original contour.

A literature search for previous experimentation with this type of tube used as a foldable member yielded reports on only the two investigations

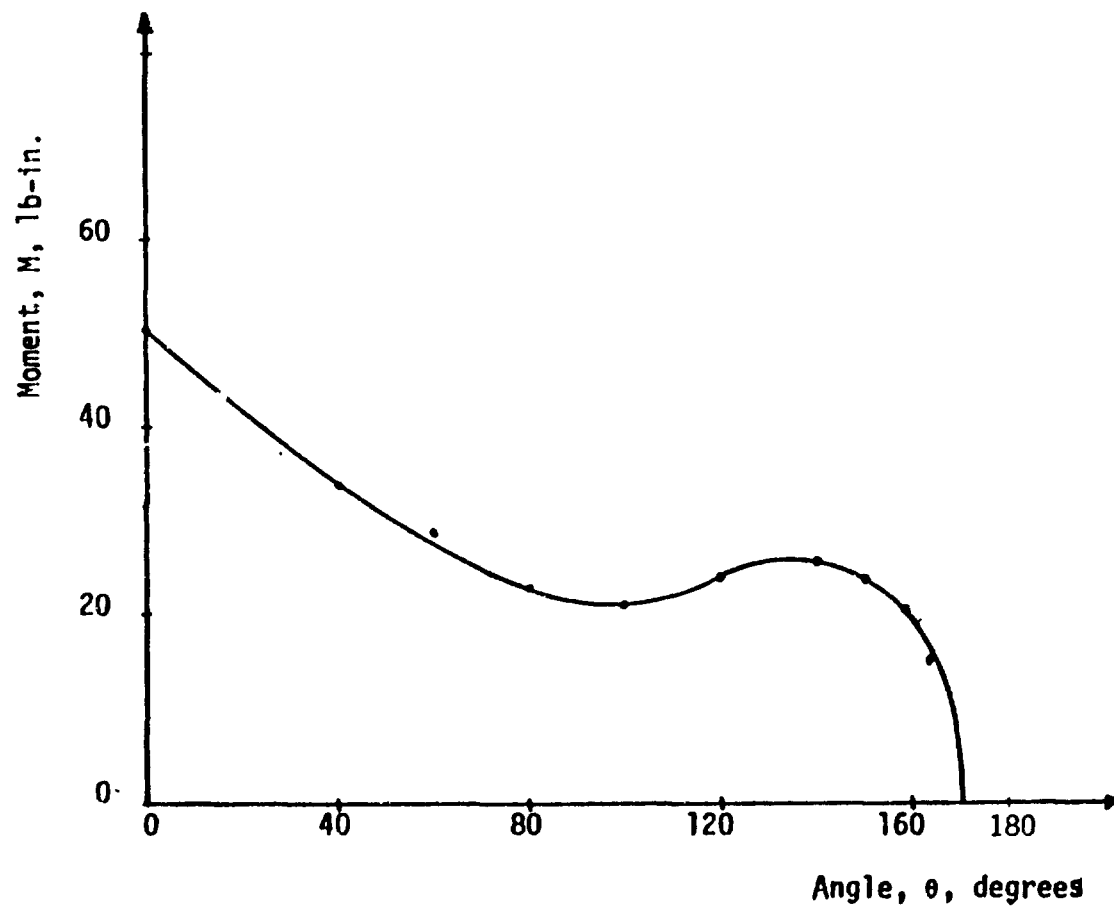


Fig. 4.1 Typical Plot of Bending Moment in lb-in. versus Angle
in degrees during deployment to slightly buckled state

cited earlier. One was conducted at NASA Lewis Research Center in 1965 (ref. 3), and the other was the research conducted for the European Space Research Organization and reported in 1973 (ref. 5.).

4.2 Deployment Test Procedure

The modified BFET's were tested using the same procedure that was used previously. The order in which the three configurations were tested was established on the basis of their rankings as structural members, aside from consideration of deployment. On this basis, the free-edged tubes were tested first since they had the least amount of lost bending stiffness due to the incisions, and the single-slotted and double-slotted followed in turn. It was at first believed that the stiffness losses in the latter two types due to the slots would be insignificant, but as is shown later, this was not the case.

The first test run on a new specimen consisted, as before, of the eight steps listed below. Steps five through eight were repeated for any subsequent tests run on the same specimen.

- (1) Installation of Wood Inserts
- (2) Attachment of End Plates
- (3) Mounting in the Testing Machine
- (4) Setting up the x-y Recorder
- (5) Folding of Specimens (accomplished as a two-step process-
collapsing then bending)
- (6) Setting of Angular Velocity
- (7) Releasing the Specimen to Unfold
- (8) Measurement of Strain Energy Using Planimeter

5. TEST RESULTS

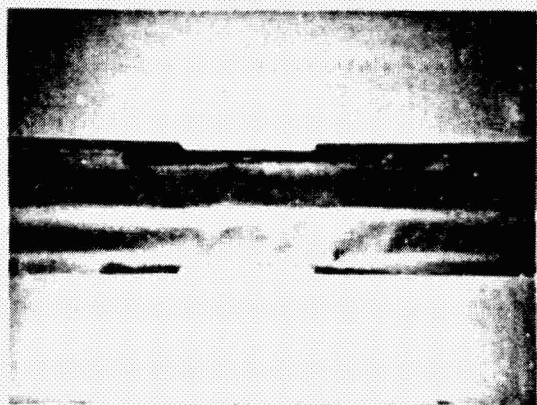
5.1 Free-Edged Tube

The specimens cut into this configuration were those indicated in Table 2.1 by "FE". Seven such specimens were cut after some preliminary trials on one specimen indicated that this innovation might work. Pairs of specimens with very similar contours were selected from Table 2.1, one of each pair to be cut into the free-edged shape and the other into the slotted configuration, so that performance comparisons could be made. However, after several of the free-edged specimens failed to completely deploy, it was clear that this design was not a reliable one and it was abandoned.

5.2 Single-Slotted Tube

After it was determined that the free-edged tube was not a viable design, attention was focused on the single-slotted tube. The specimens that were modified into this configuration are those noted by "SS" in Table 2.1. In all, 17 specimens of this type were prepared and tested, after preliminary tests on two specimens gave indication that this type of tube would deploy on successive attempts. Fig. 5.1 shows this and the other two configurations.

An incremental approach was taken in setting the dimensions of the slots so that optimum length and width could be found and no unnecessarily large cuts would be made. The slots were first cut 1/16 inch wide and 8 inches long. Tests on several specimens with this form indicated that, while they would fully deploy in a majority of cases, in other cases they would not. Even when they did unfold completely, the slot would close when the specimen was folded up, and the edges of the slot would butt together as the specimen was undergoing the unfolding action, all the way to the point where the center section was snapping back out to the original shape. This negated the function of the slot as a compressive stress alleviating device. The moment-versus-angle curve obtained from a typical specimen of this type is shown as Fig. 5.2, where the



a. Free-Edged Tube



b. Single Slotted Tube



c. Single-Slotted Tube

Fig. 5.1 Typical Modified BFET Test Specimens

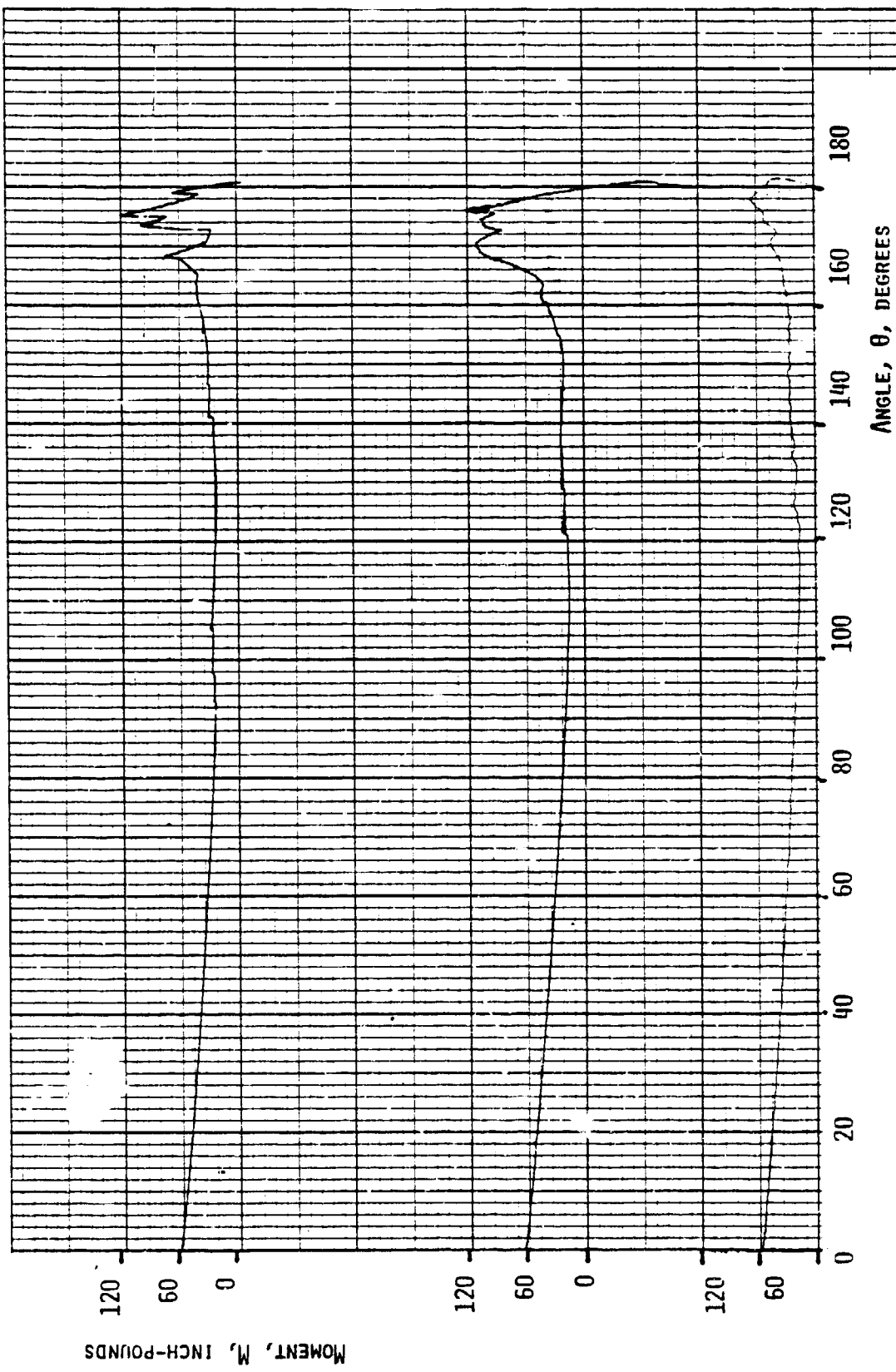


FIG. 5-2 BENDING MOMENT IN IN-LBS VERSUS ANGLE IN DEGREES FOR VARIOUS RATES OF DEPLOYMENT
SPECIMEN NE - 1, SLOT WIDTH = 1/16 INCH

ORIGINAL PAGE IS
OF POOR QUALITY

jagged part of the curve indicates resistance due to the rubbing of the slot edges against each other. It was also observed that only about a four inch length of the tube, in the center, comprised the folded region of the specimen.

In view of the above observations, the central four inches of the slots were widened by a small amount at a time to produce the slot shape shown in Fig. 5-3. The slot in each specimen was incrementally widened until a smooth

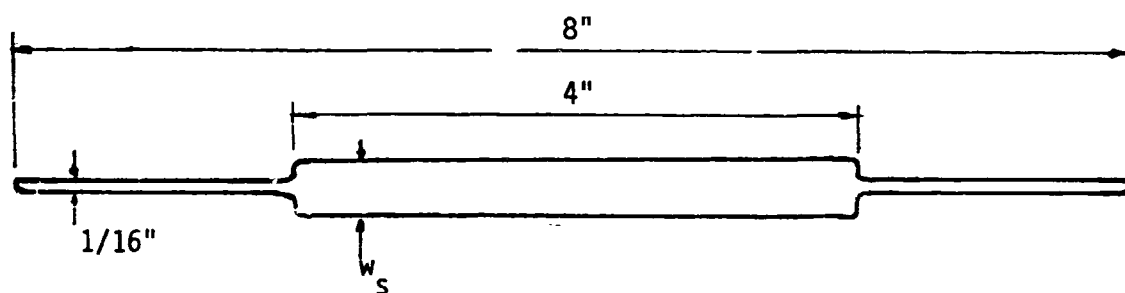


Fig. 5.3 Slot Configuration

deploying action was achieved. The final widths of the slots ranged between $\frac{1}{4}$ inch and $\frac{7}{16}$ inch. The required width turned out to be approximately inversely proportional to the specimen flatness, but bore no discernable relationship to any other parameters, at least within the range of specimen sizes tested. The approximate relation for slot width w_s was:

	$f \sim 0.8:$	$w_s \sim \frac{1}{4}"$
For $1.5 < R < 6$, and	$f \sim 0.6:$	$w_s \sim \frac{3}{8}"$
	$f \sim 0.4:$	$w_s \sim \frac{7}{16}"$

The moment-versus-angle ($M-\theta$) curves for selected specimens of each group (NA through NH) are shown in Figs. 5.4 through 5.11. These curves have the characteristic shape for the strain energy deployable member. The moment decreases gradually from its initial value as the curvature in the folded region decreases, and then as the center section expands, increasing the moment of inertia, the moment rises to a peak, then goes to zero as the tube is fully extended. The curves of Figs. 5.4 to 5.11 show the behavior of specimens in the order of increasing roundness, and it can be noted that the smooth curves depicting the behavior of the very flat and moderately flat specimens, Figs. 5.4 to 5.9, are followed by more jagged curves for the rounder shapes. This was because the snapping through of the latter contours was more sudden and vigorous, with the peaks in the curve representing the snapping through of small dimpled areas of the specimen.

5.3 Double-Slotted Tube

During experimentation with the single-slotted tube, it became apparent that the width of slot required was great enough to have a measurable affect on the bending stiffness. Calculations indicated that the loss of bending stiffness ranged between 5.5% and 23% due to removal of material at the extreme fiber of the cross-section (See Table 5.1). This result led to investigation of the double-slotted tube as a type that may deploy as well and retain a greater amount of the original bending stiffness. Research on two tubes, NC-3 and NH-1, with quite different dimensions has shown that this type deploys successfully if the total width of the two slots is the same as the slot width of a comparable single-slotted tube; i.e., with two slots, arranged symmetrically on each (compression and tension) side and each having width $1/2 w_s$. No quantitative data were acquired on strain energy released in the double-slotted tube, but experience has shown that if the tube deploys, the

strain energy will not vary significantly whether the tube has one or two slots. Therefore, the quantitative material in the next section, acquired from single-slotted tubes can be applied to the double-slotted tube as well. This type is probably the more desirable with all factors considered; the bending stiffness loss due to slotting is only one-fourth of that for the single-slotted tube.

5.4 Approximate Strain Energy-Geometry Relationship

The amounts of strain energy released in deploying the single-slotted tube specimens in this test program can be summarized as follows: The mean value for all specimens was 150 lb-ins while the range of values was $125\# \leq U \leq 176\#$. This was the result for a range of specimen properties of $1.9" < R < 5.9"$ and $0.10 < f < 0.89$, arc radius and flatness respectively.

As a final task in the investigation, an effort was undertaken to generalize the results stated above by developing, from a statistical analysis, an approximate mathematical expression relating strain energy to the two independent variables R and f . Various functional forms were tested for relative accuracy, with multiple regression analyses performed using the IBM Statistical Analysis Package containing the multiple regression subroutine MULTR. This work is detailed in ref. 9.

The form producing the best fit with the experimental data was the following:

$$U = U_0 \left\{ \frac{R}{R_0} \right\}^{\alpha} (1 - f)^{\beta} \quad \text{Eqn. 5.1}$$

where:

U = predicted strain energy

U_0 = strain energy for a reference tube ($R = R_0$, $f = 0$)

α = exponent for energy dependence on radius

β = exponent for energy dependence on flatness

The analysis yielded the following:

$$U = 142 \left\{ \frac{R}{R_0} \right\}^{0.24} (1-f)^{0.18} \quad \text{Eqn. 5.2}$$

with $R_0 = 1$ inch or equivalent. As a measure of goodness-of-fit, the index of determination was calculated as $r = 0.47$, indicating that Eqn. 5.2 should be accurate to within about 13 lb-ins.

5.5 Some Design-Related Parameters as Approximated by the Formula

A plot of predicted strain energy versus the cross-section parameters R and f is given in Fig. 5.12. Calculations relating predicted strain energy to bending stiffness and then to the member linear density were developed from Eqn. 5.2 and the following formulas:

Weight per unit length:

$$w = 8 \rho R \phi t \quad \text{Eqn. 5.3}$$

where:

w = weight per unit length

ρ = material density

R, ϕ, t = defined in Fig 2.1a

and

$$I_{\lambda} = 2R^3 t \left[4\phi - 3\sin 2\phi + 2\phi (2\cos \phi - 1)^2 \right] \quad \text{Eqn. 5.4}$$

Plots of these quantities are shown in Fig. 5.13 and Fig. 5.14.

Fig. 5.13 shows the range of choices for combinations of cross-sectional properties to produce a given required strain energy, and gives indication of the "weight penalty" due to the flattened characteristic of the FET which is required for deployment capability.

DEPLOYMENT RATE,
 $\dot{\theta}$, DEGREES/SEC

0.282

MOMENT, M, INCH-POUNDS

120
60
0

5.26

120
60
0

FREE SWING

120
60
0

0 20 40 60 80 100 120 140 160 180

ANGLE, θ , DEGREES

FIG. 5-4 BENDING MOMENT IN IN-LBS VERSUS ANGLE IN DEGREES FOR VARIOUS RATES OF DEPLOYMENT
SPECIMEN NA-2

DEPLOYMENT RATE,
 $\dot{\theta}$, DEGREES/SEC

0.282

MOMENT, M, INCH-POUNDS

120
60
0

5.26

120
60
0

FREE SWING

120
60
0

0 20 40 60 80 100 120 140 160 180

ANGLE, θ , DEGREES

FIG. 5-5 BENDING MOMENT IN IN-LBS VERSUS ANGLE IN DEGREES FOR VARIOUS RATES OF DEPLOYMENT
SPECIMEN NB-1

DEPLOYMENT RATE,
 $\dot{\theta}$, DEGREES/SEC

0.282

MOMENT, M, INCH-POUNDS

5.26

FREE SWING

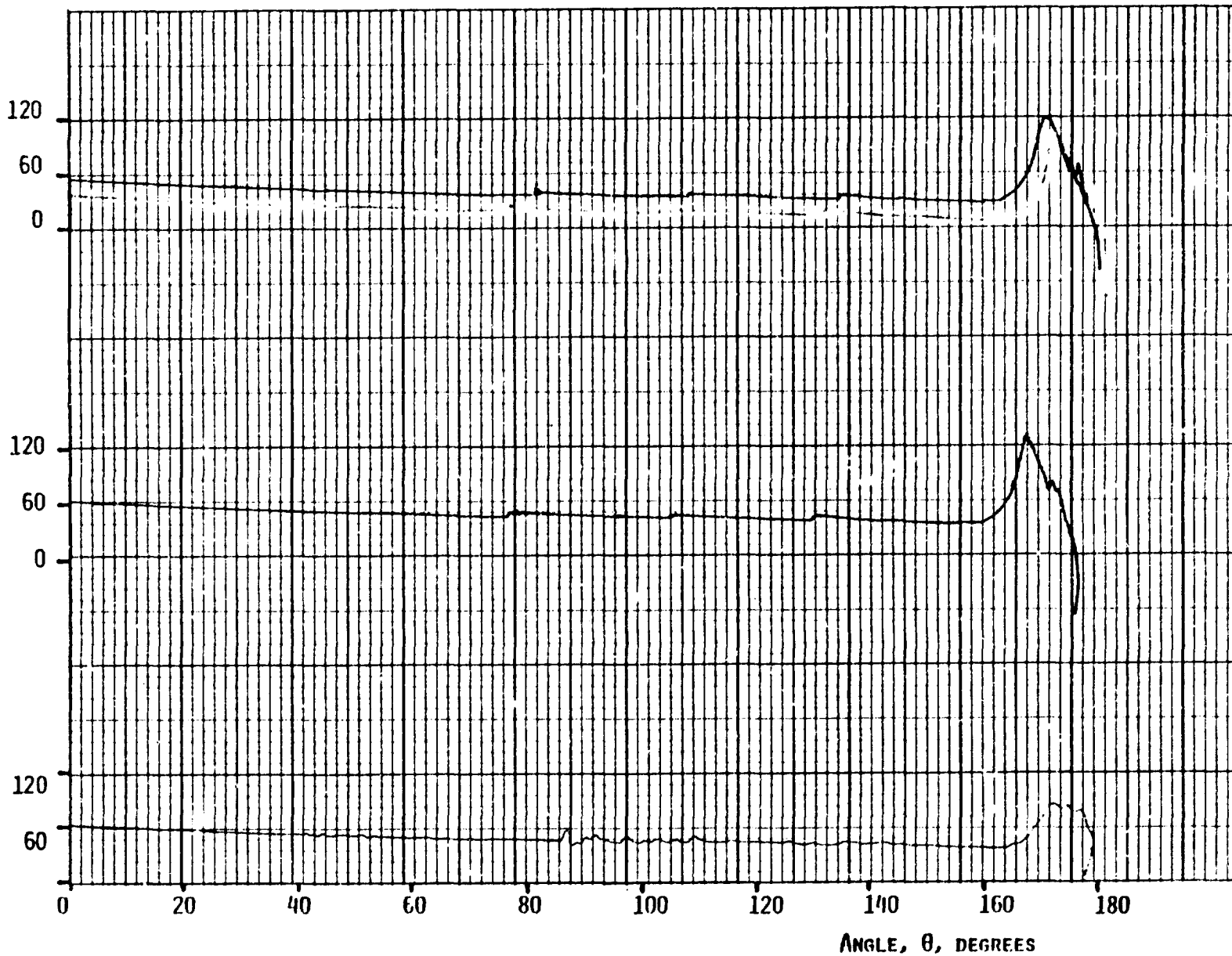


FIG. 5-6 BENDING MOMENT IN IN-LBS VERSUS ANGLE IN DEGREES FOR VARIOUS RATES OF DEPLOYMENT
SPECIMEN NC-1

DEPLOYMENT RATE,
 $\dot{\theta}$, DEGREES/SEC

0.282

MOMENT, M, INCH-POUNDS

120
60
0

5.26

120
60
0

FREE SWING

120
60
0

0 20 40 60 80 100 120 140 160 180
ANGLE, θ , DEGREES

FIG. 5-7 BENDING MOMENT IN IN-LBS VERSUS ANGLE IN DEGREES FOR VARIOUS RATES OF DEPLOYMENT
SPECIMEN ND-2

DEPLOYMENT RATE,
 $\dot{\theta}$, DEGREES/SEC

0.282

MOMENT, M, INCH-POUNDS

5.26

FREE SWING

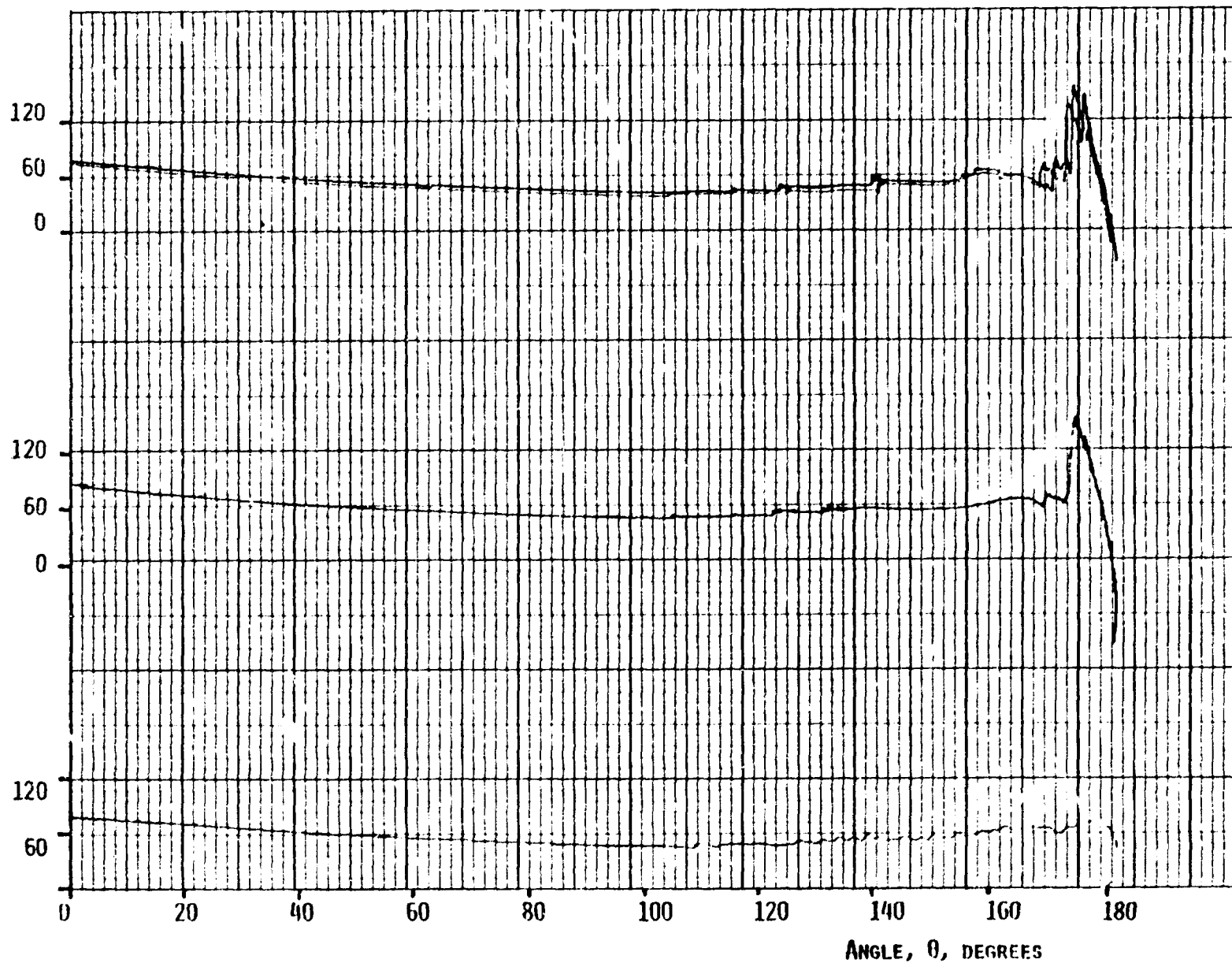


FIG. 5-8 BENDING MOMENT IN IN-LBS VERSUS ANGLE IN DEGREES FOR VARIOUS RATES OF DEPLOYMENT
SPECIMEN NE-2

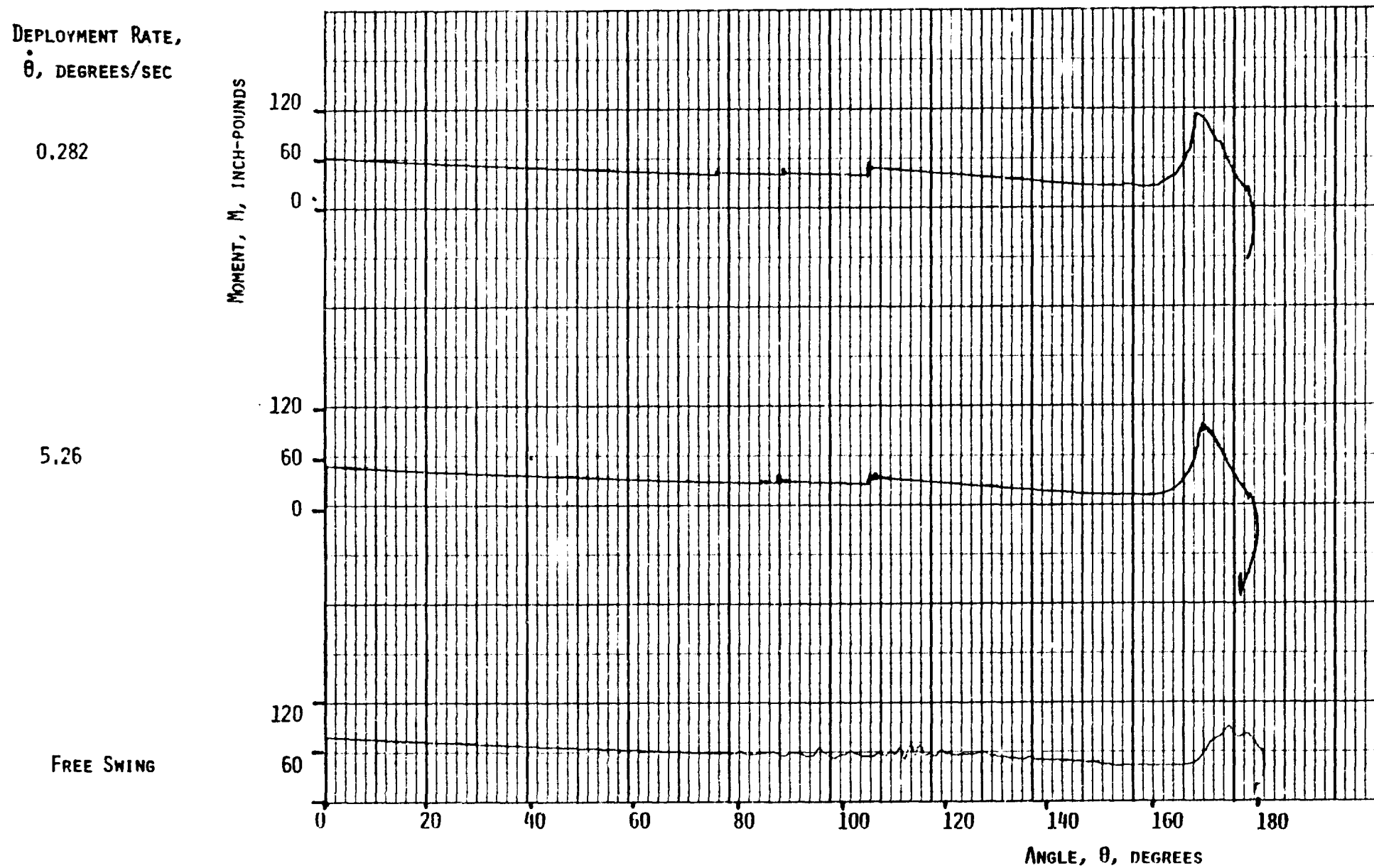


FIG. 5-9 BENDING MOMENT IN IN-LBS VERSUS ANGLE IN DEGREES FOR VARIOUS RATES OF DEPLOYMENT
SPECIMEN NF-1

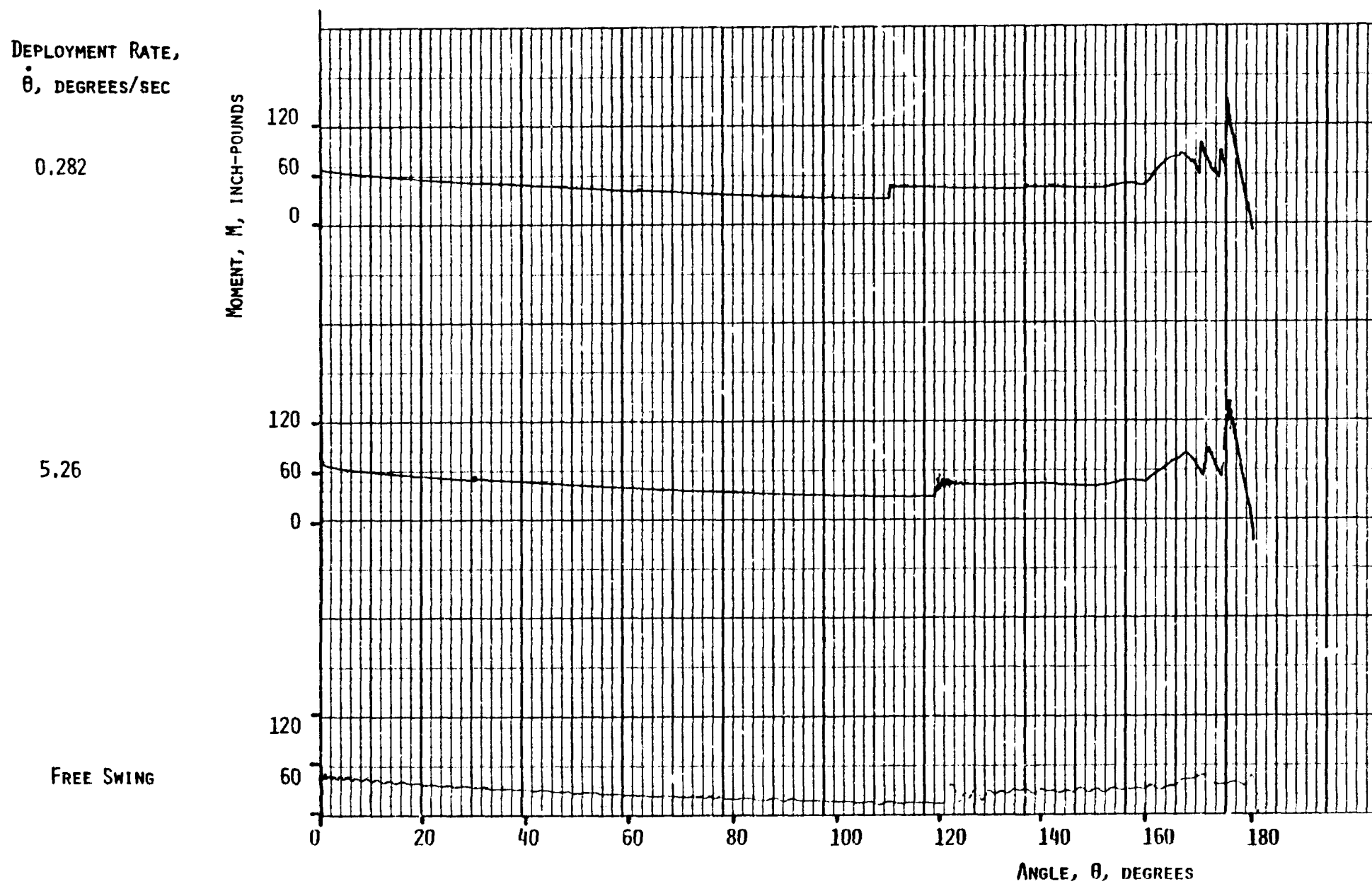


FIG. 5-10 DENDING MOMENT IN IN-LBS VERSUS ANGLE IN DEGREES FOR VARIOUS RATES OF DEPLOYMENT
SPECIMEN NG-3

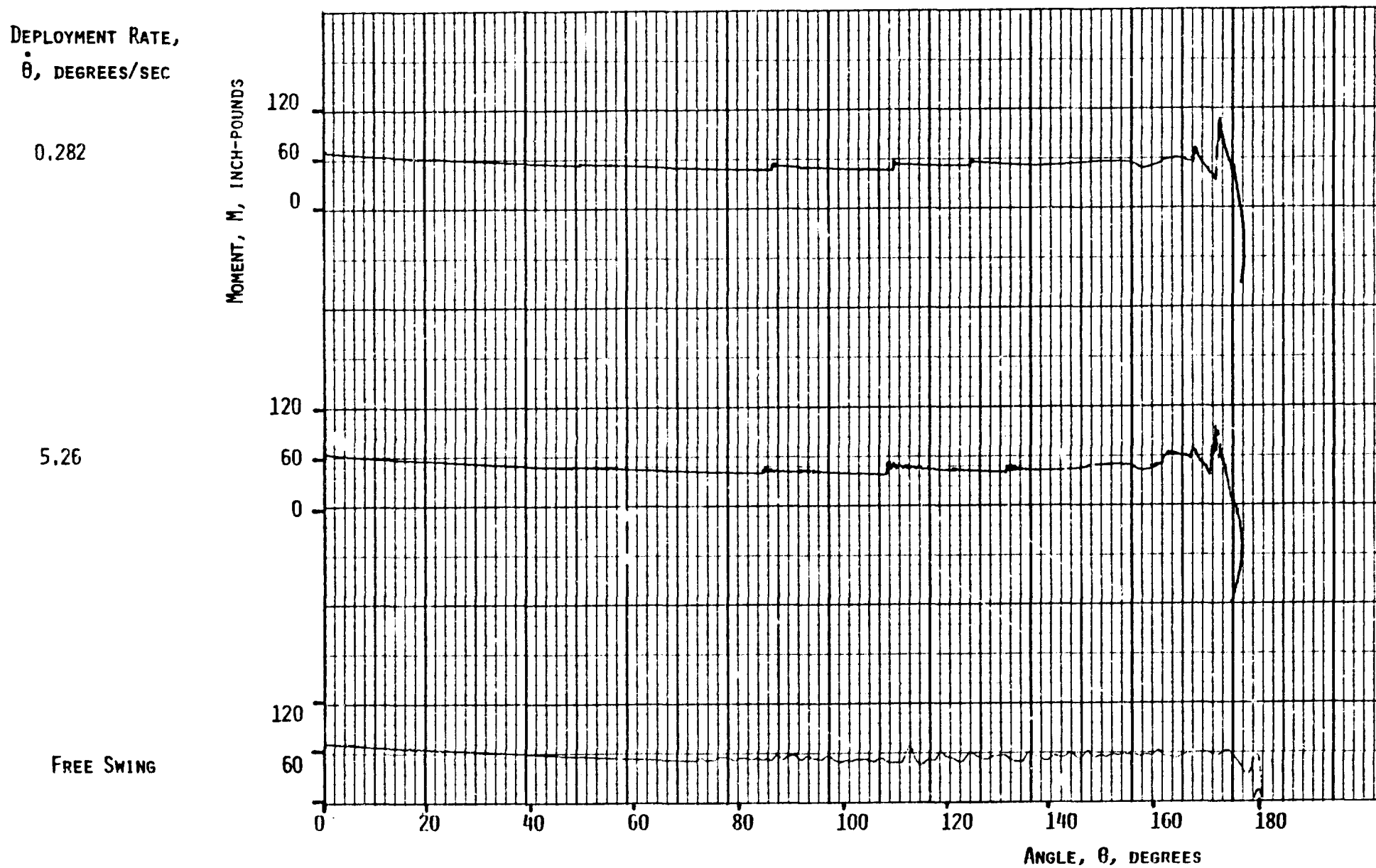


FIG. 5-11 BENDING MOMENT IN IN-LBS VERSUS ANGLE IN DEGREES FOR VARIOUS RATES OF DEPLOYMENT
SPECIMEN NH-4

TABLE 5.1

34

REDUCTION IN BENDING STIFFNESS DUE TO SLOT INSERTION
(typical specimens)

Specimen Number	Moment of Inertia Uncut Specimen, in. ⁴	Moment of Inertia Single-Slotted Spec., in. ⁴	% Difference
NA-2	0.027	0.025	8.0
NC-1	0.018	0.015	19.7
NE-2	0.155	0.135	13.0
NF-1	0.016	0.013	20.1
NH-4	0.286	0.254	11.3

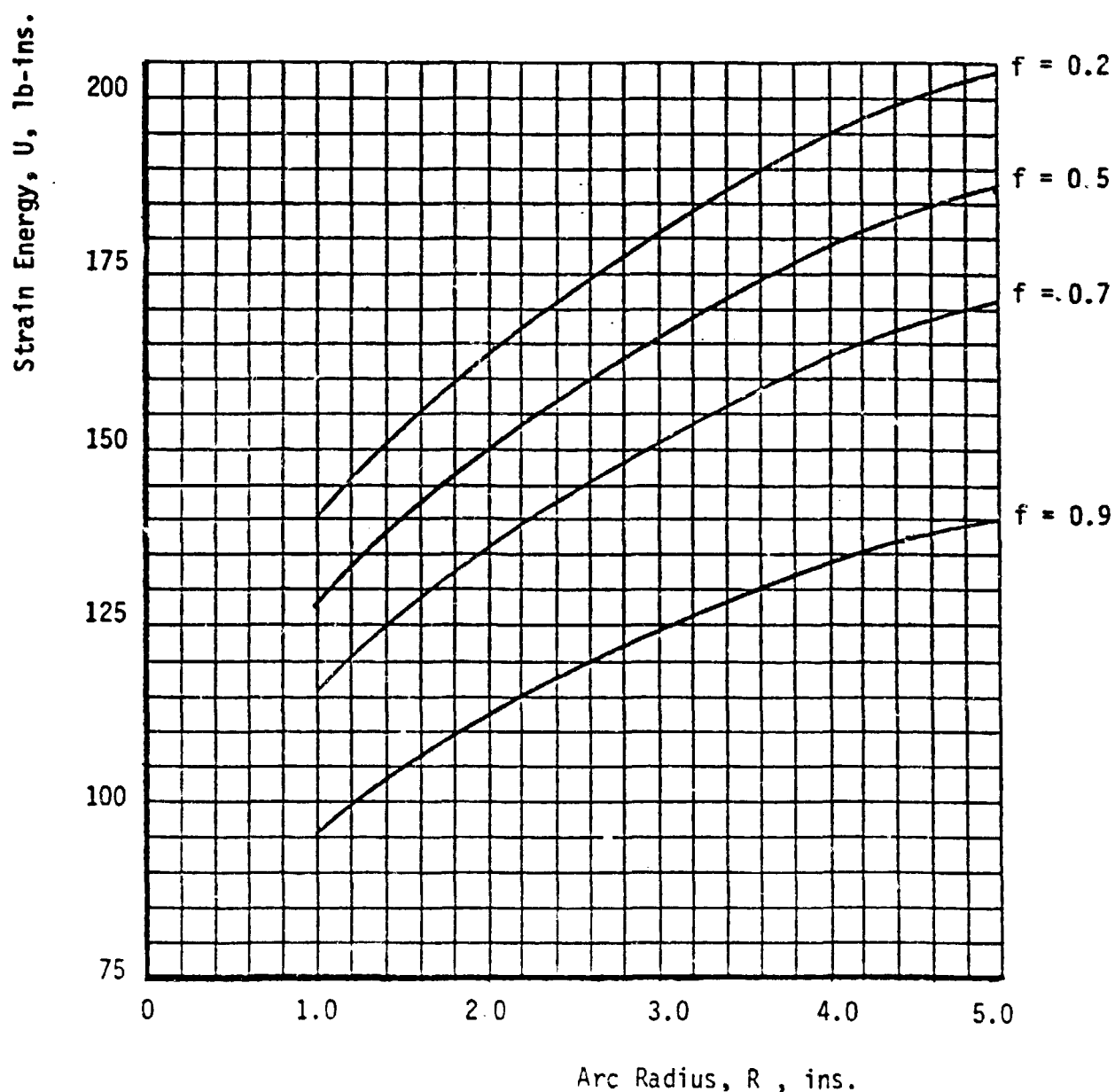


Fig. 5-12 Predicted Strain Energy (lb-ins) versus Arc Radius (ins.) for different values of the Flatness Parameter.

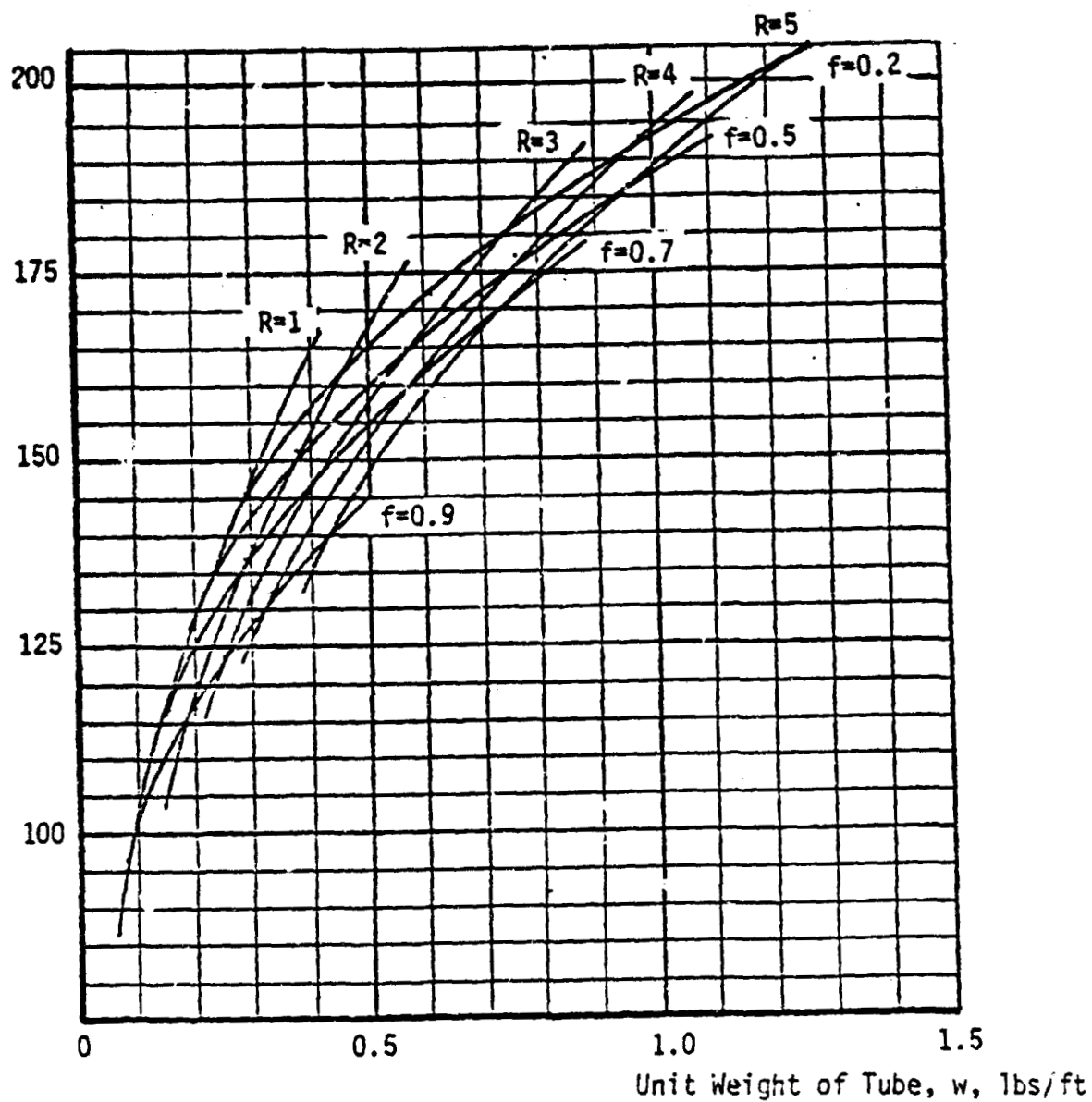
Strain Energy, U , lb-ins.

Fig. 5-13 Predicted Strain Energy (lb-ins.) versus Unit Weight of Tube (lbs/ft) for different values of Arc Radius (R) and Flatness Parameter (f)

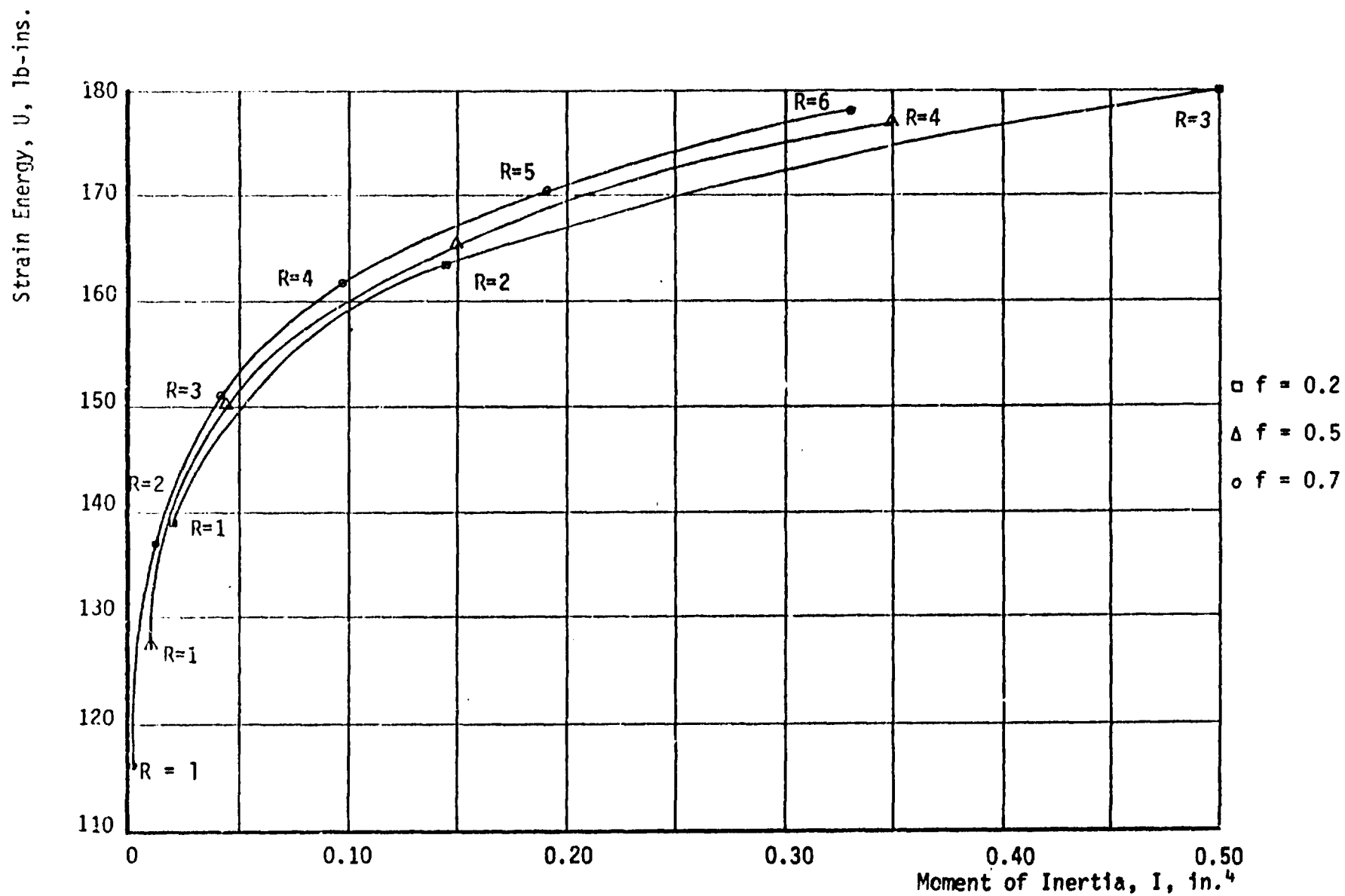


Fig. 5-14 Strain Energy (lb-ins) versus Moment of Inertia(in.⁴) for various combinations of Arc Radius (R, in.) and Flatness (f)

Fig. 5.14 indicates approximate dimensions for a tube of the material and wall-thickness used in this investigation needed to produce a required strain energy and bending stiffness.

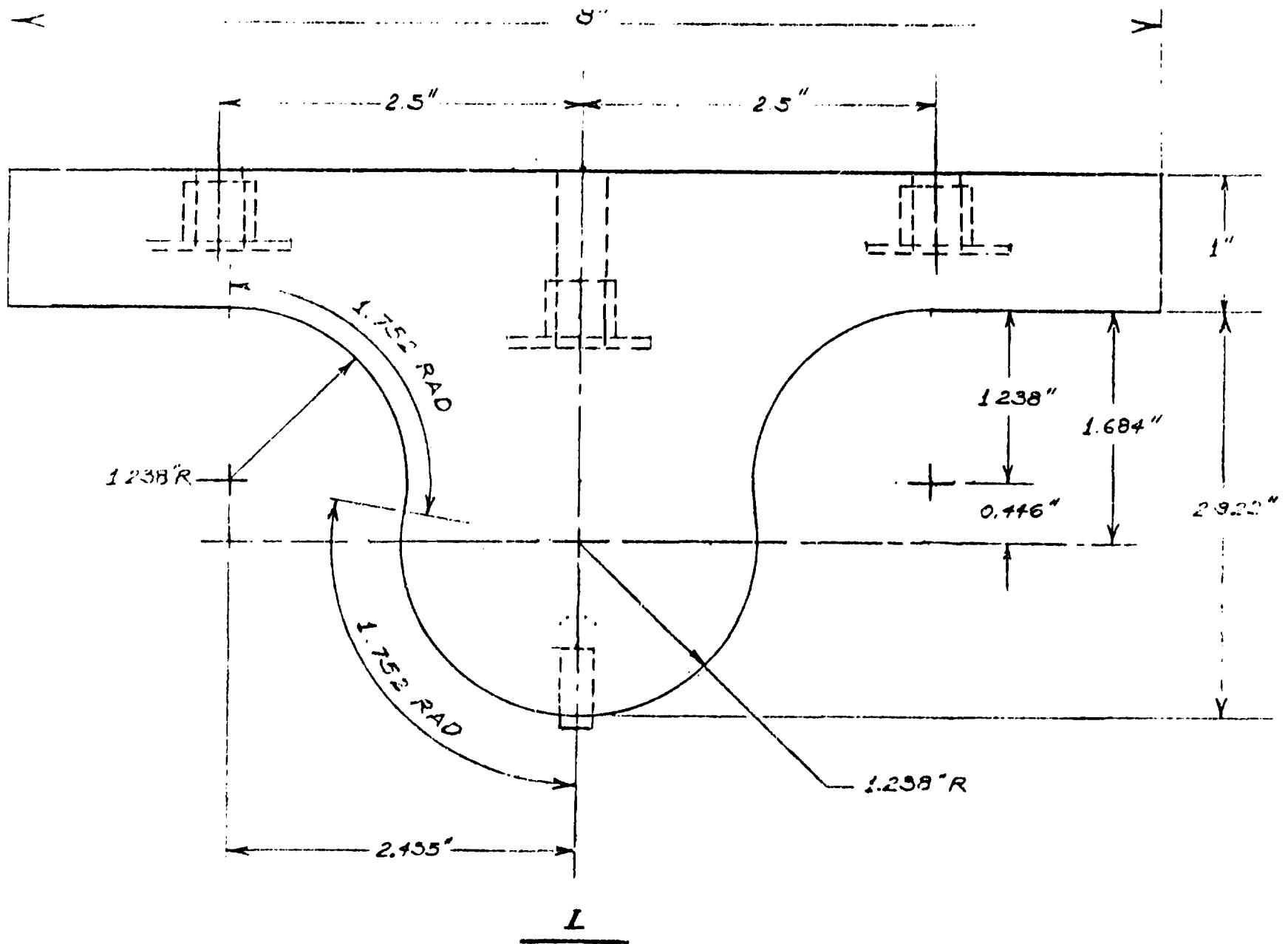
6. CONCLUSION

This investigation has demonstrated that with a certain stress alleviating device, namely, one or more slots cut longitudinally in the center, the bi-convex foldable elastic tube is a viable type of member for use in strain-energy-deployable structures. It has also shown that strain energy quantities in the range of 125# to 175# are realizable from tubes representing large space structure members in the 15' to 20' length range. Approximate strain energy/geometric parameter relationships have been developed which may be useful for preliminary design or concept studies, although their applicability is limited to the variables of this research study.

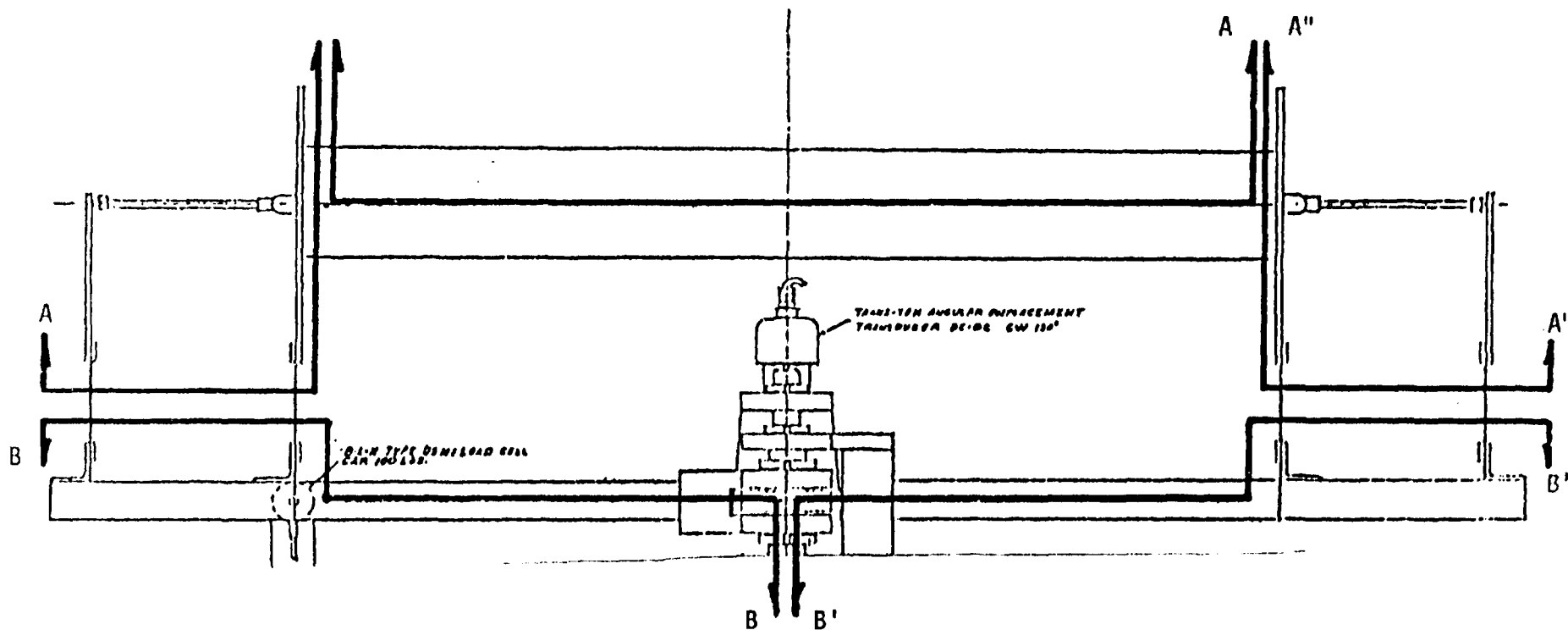
Presently, a short shell buckling test set-up is being constructed to test the tube specimens for local buckling loads. Additional design criteria for the bi-convex foldable elastic tube should result from that analysis.

REFERENCES

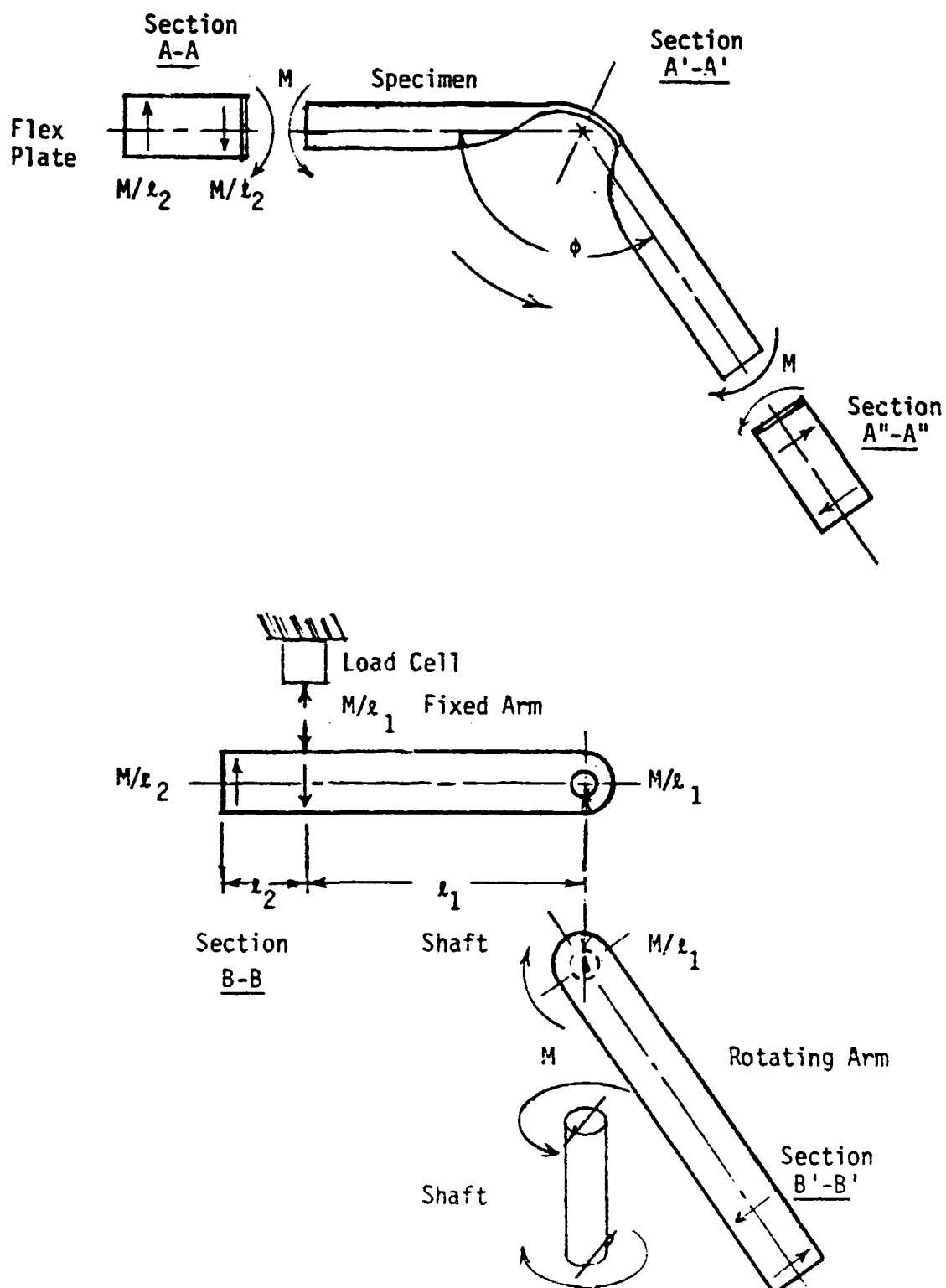
1. Jones, I.W., Boateng, C., Williams, C.D.: Foldable Elastic Tubes for Large Space Structure Applications, Final Report-Phase I, January 1980.
2. NASA-Howard University Graduate Research Program in Advanced Aerospace Structures: Status Report, January 1981.
3. Gertsma, L.W., Dunn, J.H., Kempke, E.E., Jr.: Evaluation of One Type of Foldable Tube, NASA TM X-1187, December 1965.
4. Crawford, R.F.: Strength and Efficiency of Deployable Booms for Space Applications, AIAA Paper No. 71-396, Variable Geometry and Expandable Structures Conference, April 1971.
5. Fernandez-Sintes, J., Cristos, J.C.: Foldable Elastic Tubes for Hinges on Satellites, Contractor Report ESRO-CR 65 by Instituto Nacional de Tecnica Aeroespacial, Madrid, Spain, for the European Space Research Organization, February 1973.
6. Mikulus, M.M., Bush, H.G., Card, M.F.: Structural Stiffness, Strength and Dynamic Characteristics of Large Tetrahedral Space Truss Structures, NASA TM X-74001, March 1977.
7. Product Data, Armco 17-7PH Precipitation Hardening Stainless Steel Sheet and Strip, Armco Steel Corp. Advanced Materials Division, Baltimore, Maryland.
8. Boateng, C.: Deployment Tests for One Type of Foldable Elastic Tube (BFET), Master's Degree Thesis, Howard University, December 1979.
9. Williams, C.: Experimental Evaluation of Foldable Elastic Tubes Modified with Stress Alleviating Devices, Master's Degree Thesis, Howard University, February, 1981.



APPENDIX A: TYPICAL FORM BLOCK DRAWING



HOWARD UNIVERSITY
DEPARTMENT OF CIVIL ENGINEERING
1000 UNIVERSITY AVENUE
WASHINGTON, D.C. 20004
STATIC FORCE DISTRIBUTION TESTING
MACHINE



APPENDIX B:

QUASI-STATIC FORCE DISTRIBUTION
FET TESTING MACHINE